

Photometry of seven overlooked open clusters in the First and Fourth Galactic Quadrants

G. Carraro^{1,2},[★] K. A. Janes³, E. Costa¹, and R. A. Méndez¹,[†]

¹Departamento de Astronomía, Universidad de Chile, Casilla 36-D, Santiago, Chile

²Astronomy Department, Yale University, P.O. Box 208101, New Haven, CT 06520-8101, USA

³Department of Astronomy, Boston University, 725 Commonwealth Avenue, Boston, MA 02215, USA

Submitted: Dec. 2005

ABSTRACT

CCD *BVI* photometry is presented for 7 previously unstudied star clusters projected toward the inner side of the Galaxy: Trumpler 23, Lynga 3, Collinder 307, Ruprecht 134, ESO552SC16, AL 5 and Kronberger 3. Color magnitude diagrams of the cluster regions allow us to conclude that Lynga 3 and ESO552SC16, are not clusters, but groups of bright stars probably located in the Carina-Sagittarius spiral arm. AL 5 and Kronberger 3 are so embedded in a dense stellar field that we cannot confirm their nature. Trumpler 23 and Ruprecht 134 are two intermediate-age open clusters located well inside the solar ring which deserve further attention.

Finally, Collinder 307 is an obscured younger cluster (250 Myr) located in the Carina-Sagittarius spiral arm. Our results emphasize the difficulty to search for open clusters in the inner regions of the Galaxy due to the richness of the field and the patchy nature of the interstellar absorption, but at the same time significantly contribute to a better understanding of this complicated regions of the Milky Way.

Key words: Open clusters and associations: general – open clusters and associations: individual: Trumpler 23, Lynga 3, Collinder 307, Ruprecht 134, ESO552SC16, AL 5, Kronberger 3.

1 INTRODUCTION

This paper is the third of a series (Carraro et al. 2005a,b) aimed at increasing the sample of open clusters studied in the First and Fourth Galactic Quadrants. This is a very complicated and barely known region of the Galaxy due to the highly variable extinction pattern and the extreme richness of the Galactic disk and bulge fields.

In particular the existence and survival of intermediate-age open clusters in this region of the Galaxy is very difficult, and indeed the vast majority of intermediate-age clusters is found in the anti-center direction (Janes & Phelps 1994). Inside the solar ring the Galactic tidal field is very strong and as a consequence star clusters dissolve more rapidly than in the other regions of the Milky Way disk. In Carraro et al. (2005a) we discussed NGC 6404 and NGC 6583, and found that they are intermediate-age clusters located inside the solar circle. This combination of age and position is very

interesting due to low survival rate of star clusters in these regions. In Carraro et al. (2005b) we studied 8 candidate clusters, and found that only 3 are physical groups, namely AL 1, Berkeley 80 and NGC 5764, thus emphasizing the difficulties inherent in studying the stellar populations toward the inner regions of the galaxy.

The final goal of this survey is to find intermediate-age clusters inside the solar circle, which will allow us to enlarge the baseline of the radial abundance gradient holding for the Galactic disk (Friel 2002) and to improve the open cluster age distribution (Carraro et al. 2005c). At the same time these clusters, in the event they turn out to be young, will help to better delineate the spiral structure inside the solar circle.

In this paper we present the first CCD photometric study of seven candidate open clusters, namely Trumpler 23, Lynga 3, Collinder 307, Ruprecht 134, ESO552SC16, AL 5, and Kronberger 3 with the aim to clarify their nature and provide estimates of their fundamental parameters. None of these clusters have been studied so far, but for Collinder 307 (Moffat & Vogt 1975).

[★] Andes Fellow, on leave from Dipartimento di Astronomia, Università di Padova, Vico Osservatorio 2, I-35122, Padova, Italy

[†] email: gcarraro@das.uchile.cl (GC), , janes@bu.edu (KAJ), costa@das.uchile.cl (EC), rmendez@das.uchile.cl (RAM)

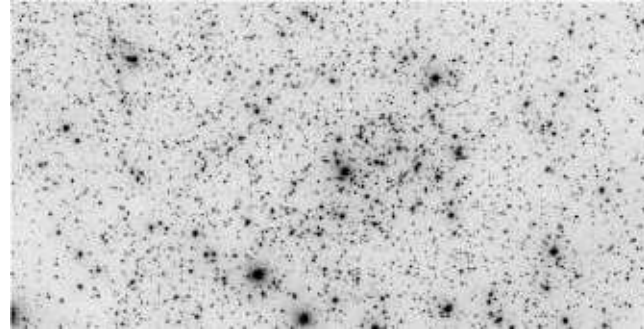


Figure 1. I band image of Trumpler 23. North is up, East to the left

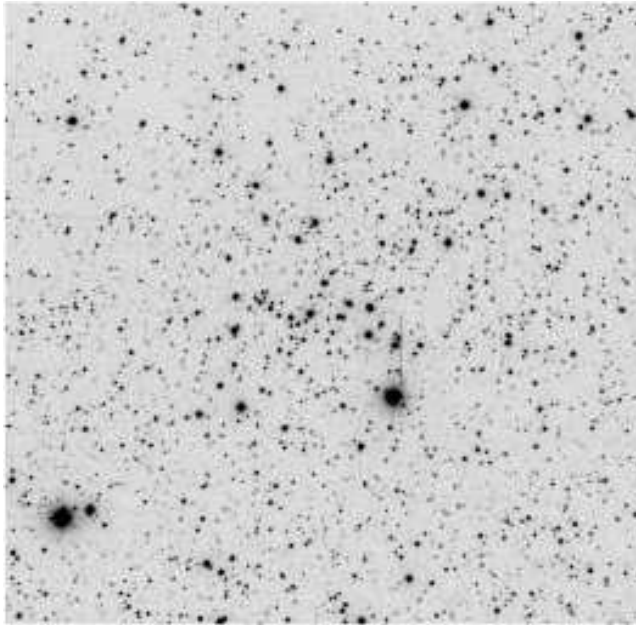


Figure 2. I band image of Lynga 3. North is up, East to the left.

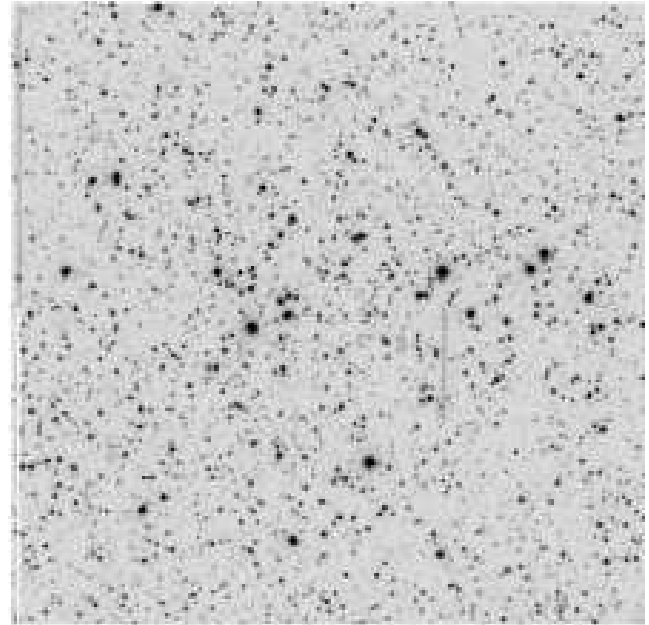


Figure 3. I band image of Collinder 307. North is up, East to the left.

Table 1. Basic parameters of the clusters under investigation. Coordinates are for J2000.0 equinox and have been visually re-determined by us.

Name	RA	DEC	<i>l</i>	<i>b</i>
	<i>hh : mm : ss</i>	$^{\circ} : ' : ''$	[deg]	[deg]
Lynga 3	15:12:36	-58:08:00	321.03	-0.64
Trumpler 23	16:00:50	-53:31:23	328.83	-0.43
Collinder 307	16:35:20	-51:00:00	334.41	-2.31
Ruprecht 134	17:52:43	-29:33:00	0.27	-1.64
ESO552SC16	18:19:05	-27:07:48	5.21	-5.54
AL 5	18:44:19	-04:55:48	27.73	-0.67
Kronberger 3	19:39:00	+06:46:00	44.46	-7.38

the observation and reduction strategies. Sect. 3 deals with the Color-Magnitude Diagrams (CMD) and illustrates the derivation of the clusters' fundamental parameters. Finally, Sect. 4 provides a detailed discussion of the results.

2 OBSERVATIONS AND DATA REDUCTION

The data presented in this paper have been collected during three observing runs at Las Campanas (LCO), Cerro Tololo (CTIO) and La Silla (LSO) Observatories, Chile.

2.1 Las Campanas observations: Trumpler 23

VI observations were carried out with the eight CCD mosaic camera on-board the 1.3m Warsaw telescope at LCO (Chile), on the night of April 4, 2005. The cluster was centered in chip #3. With a pixel size of $0''.26$, and a CCD size of 4096×2048 pixels, this samples a $17'.7 \times 8'.9$ field in the sky.

Fig. 1 shows the finding chart in the area of Trumpler 23. North is up, and East on the left.

The cluster coordinates were re-determined by us on a visual inspection basis (see Table 1). The data have been re-

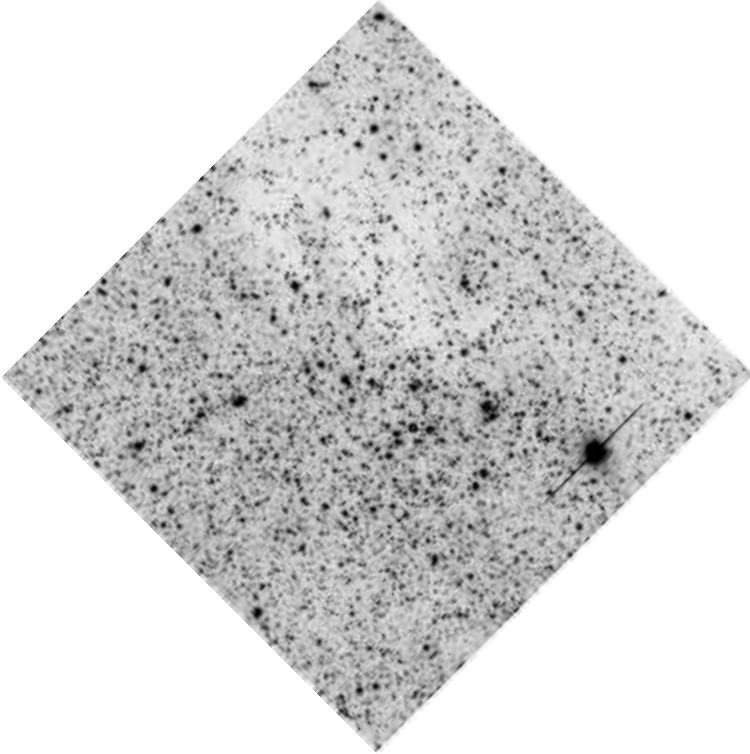


Figure 4. V band image of Ruprecht 134. North is up, East to the left.

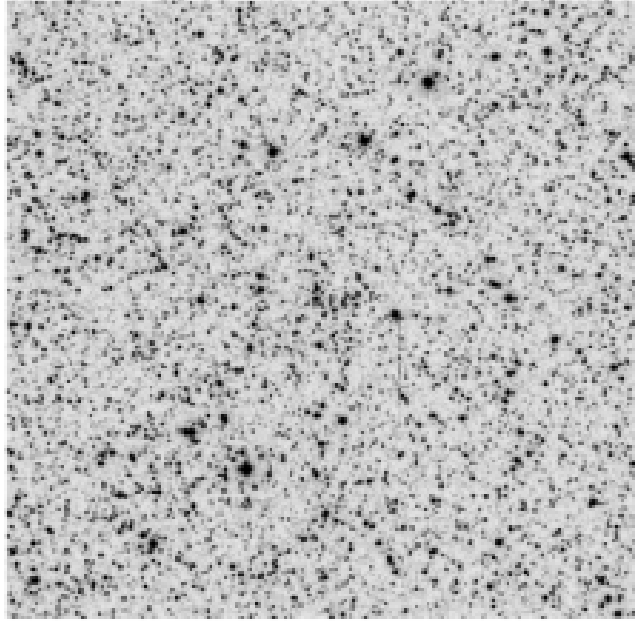


Figure 5. I band image of ESO552SC16. North is down, East to the left.

duced with the IRAF[‡] packages CCDRED, DAOPHOT, ALLSTAR and PHOTCAL using the point spread function (PSF) method (Stetson 1987). The night turned out

[‡] IRAF is distributed by NOAO, operated by AURA under cooperative agreement with the NSF.

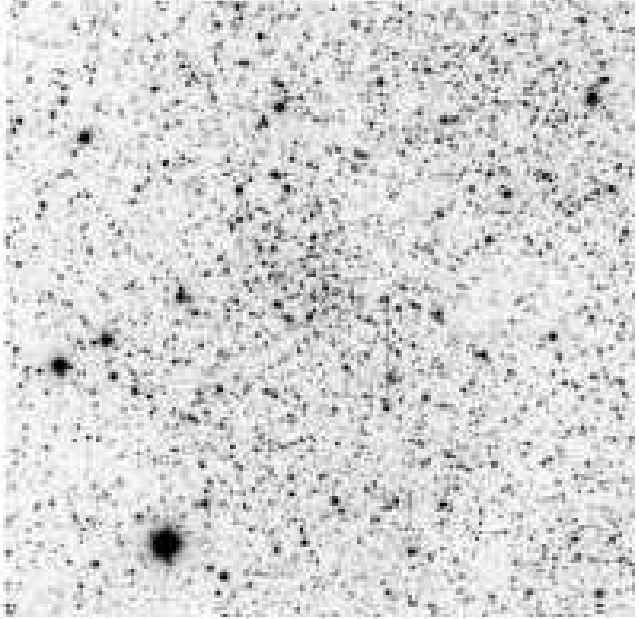


Figure 6. I band image of AL 5. North is up, East to the left.

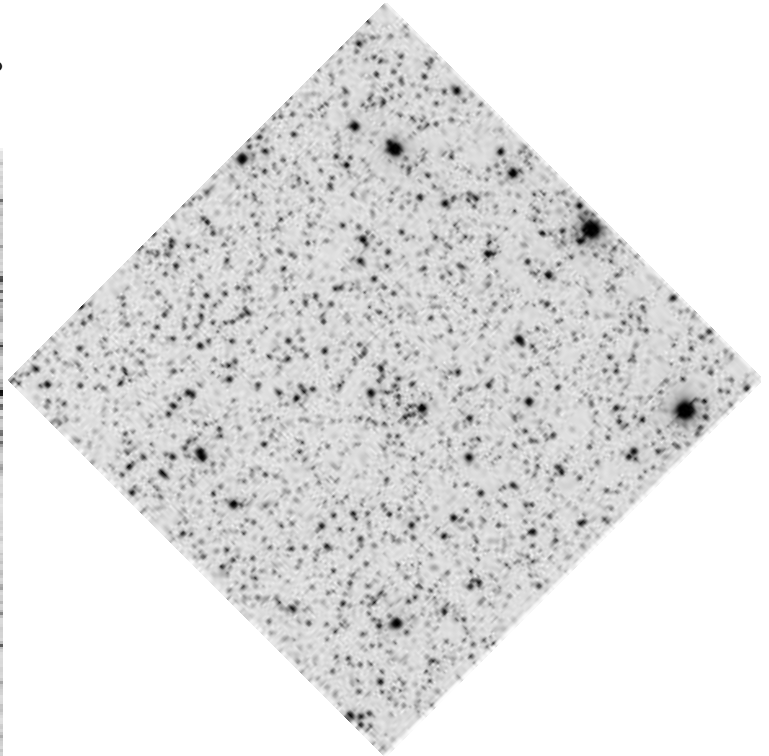


Figure 7. V band image of Kronberger 3. North is up, East to the left.

to be photometric, and we derived calibration equations for 98 standard stars observed during the night in the Landolt (1992) fields SA 104-334, PG 0942-029, SA110-362, SA 100-269, SA 101-268, G12-43 and SA 107-601.

The calibration equations are of the form:

$$v = V + (2.206 \pm 0.005) + (0.15 \pm 0.02) \times X - (0.033 \pm 0.006) \times$$

$$(V - I) \\ i = I + (2.542 \pm 0.005) + (0.10 \pm 0.02) \times X + (0.085 \pm 0.006) \times (V - I),$$

where VI are standard magnitudes, vi are the instrumental ones and X is the airmass. The standard stars in these fields provide a very good color coverage being $-0.5 \leq (V - I) \leq 3.25$. The final *r.m.s.* of the calibration are 0.018 and 0.023 for the V and I filter, respectively. Photometric errors have been estimated following Patat & Carraro (2001, appendix A). It turns out that stars brighter than $V \approx 21$ mag have global photometric errors (DAOPHOT internal plus calibration errors) lower than 0.20 mag in magnitude and lower than 0.28 mag in colour at $V = 21$ mag.

2.2 CTIO observations: Lynga 3, AL 5, Collinder 307 and ESO552SC16

VI photometry of fields in the region of Lynga 3, AL 5, Collinder 307 and ESO552SC16 was obtained at the CTIO 1.0m telescope on June 8 2005, and at the 0.9m telescope on the nights of 2 and 3 July 2005. The night of June 8 was not photometric, and we took short (5 sec) and deep exposures (300 sec). The reduction of these data followed Carraro et al. (2005b) and were calibrated using the 0.9m observations of July 2 and 3. The pixel scale of the 0.9m 2048×2046 Tek2k #3 CCD is $0.396''$, yielding a field of 13.5×13.5 arcmin on the sky. The two nights were photometric with an average seeing of 2.0 and 1.5 arcsec, respectively. We took only short (10 to 80 secs) exposures in all the filters to avoid saturation of the brightest stars.

Calibration was secured through the observation of Landolt (1992) standard fields G 14, G 26, PG 1525, PG 1323, SA 110, and SA 112 for a grand total of 86 standard stars. The calibration equations have the form:

$$v = V + (2.006 \pm 0.006) + (0.15 \pm 0.01) \times X + (0.023 \pm 0.006) \times (V - I) \\ i = I + (2.864 \pm 0.009) + (0.09 \pm 0.01) \times X + (0.034 \pm 0.007) \times (V - I),$$

and the final *r.m.s.* of the calibrated data (fitting plus calibration) turn out to be 0.022 and 0.025 for the V and I the pass-bands.

Stars brighter than $V \approx 20$ mag have global photometric errors (DAOPHOT internal plus calibration errors) lower than 0.30 mag in magnitude and lower than 0.35 mag in colour.

2.3 La Silla observations: Ruprecht 134 and Kronberger 3

BV photometry of fields in the region of Ruprecht 134 and Kronberger 3 was taken at the Danish 1.54m telescope on September 20 2005. The Danish telescope 2048×2048 CCD has a pixel scale of $0.395''$, giving a field of 13.5×13.5 squared arcmin in the sky. The reduction of this data followed Carraro et al. (2005b). The night was photometric with an average seeing of 1.5 arcsec. We took short and deep exposures (10 to 600 secs) exposures in all the filters to avoid saturation of the brightest stars.

Calibration was secured through the observation of Landolt (1992) standard fields MarkA, TPhoenix, PG0231 and PG2213 for a grand total of 56 standard stars. The calibration equations turned out to be of the form:

$$b = B + (0.752 \pm 0.006) + (0.22 \pm 0.01) \times X - (0.083 \pm 0.006) \times (B - V) \\ v = V + (0.280 \pm 0.006) + (0.18 \pm 0.01) \times X - (0.005 \pm 0.006) \times (B - V)$$

and the final *r.m.s.* of the calibrated data (fitting plus calibration) turn out to be 0.032 and 0.025 for the B and V the pass-bands.

Stars brighter than $V \approx 21$ mag have global photometric errors (DAOPHOT internal plus calibration errors) lower than 0.30 mag in magnitude and lower than 0.35 mag in colour.

For all the clusters we performed a completeness analysis, following the prescriptions described in Carraro et al. (2005d).

The final photometric data (X and Y coordinates, magnitudes and errors) consist of 6000, 11225, 7979, 11995, 22729, 13347 and 6553 stars in Lynga 3, Trumpler 23, Collinder 307, Ruprecht 134, ESO552SC16, AL 5, and Kronberger 3, respectively, and are made available in electronic form at the WEBDA[§] site maintained by E. Paunzen.

3 COLOUR-MAGNITUDE DIAGRAMS AND CLUSTER PARAMETERS

In this section we describe cluster CMDs and derive their basic parameters.

We first evaluated the CMD data as well as images from the 2-Micron All Sky Survey (2MASS) all sky data release (available at www.ipac.caltech.edu/2mass/releases/allsky) to explore the existence of the clusters as physical systems. The 2MASS K_s images are substantially less affected by reddening than the visual images which means that in some cases, the confusion from background galactic stars can be higher, but the background should often also be less variable.

Distance moduli, reddenings and ages of the confirmed clusters have been derived by matching by eye the observed CMDs to isochrones from the Padova group (Girardi et al. 2000), paying particular attention to the shape of the Main Sequence (MS), the position of the brightest MS stars, the turn-off point (TO) and the mean location of evolved stars, if present.

To infer the heliocentric distances we adopted $R_V = A_V/E(B - V) = 3.1$.

The results are summarized in Table 2, where the basic parameters are listed together with their uncertainties. The latter correspond to the shift allowed to isochrone fitting before a mismatch is clearly perceived by eye inspection.

[§] <http://univie.ac.at/webda/navigation.html>

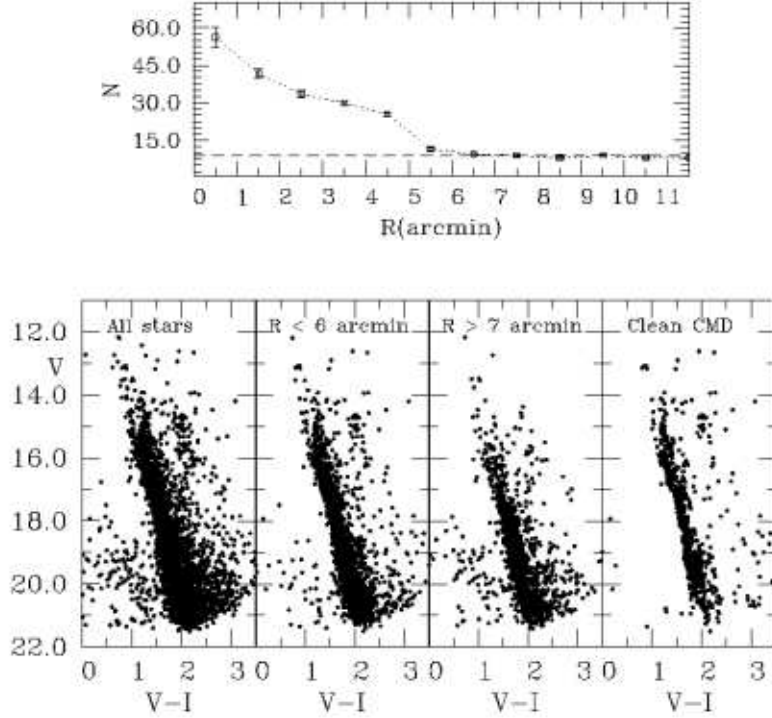


Figure 8. The open cluster Trumpler 23. The upper panel shows the radial density profile, while the lower panels, from the left to the right show the CMD of all the observed stars, and of the cluster, field and field-decontaminated cluster, respectively. See text for more details

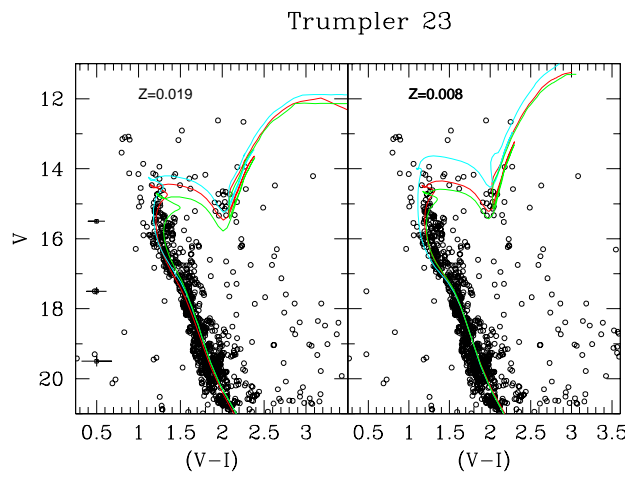


Figure 9. Isochrone solution for Trumpler 23. In the left panel isochrones of ages of 0.8, 0.6 and 0.5 Gyr (from the bottom to the top) and solar metallicity are shown. In the right panel isochrones of ages of 0.8, 0.7 and 0.5 Gyr (from the bottom to the top) and for $Z=0.008$ are shown. See text for more details.

3.1 Trumpler 23

Trumpler 23 was firstly noted by Trumpler (1929) and then by van den Bergh & Hagen (1975), who named it BH 180, and described it as a moderately populated cluster having a diameter of 6 arcmin, clearly visible both on red and on blue plates (see Fig. 1). To assess the reality of this clear over-density, we statistically cleaned the CMD following the prescriptions described in Bertelli et al. (2003). The procedure is shown in Fig. 8. The left panel presents the CMD of all the stars observed in the region of Trumpler 23. Here the MS extends from $V=15.5$ to $V=22.0$, with a TO located at $V \approx 16.0$, $(V-I) \approx 1.1$.

This MS is rather broad, substantially wider than the photometric errors at a given magnitude (see Sect. 2). We ascribe this to field star contamination, to some differential reddening and perhaps to the presence of a sizeable binary star population, which mainly enlarges the MS toward red colors. A significant over-density of stars at $V \approx 15$, $(V-I) \approx 2$ might be the signature of a Red Giant Branch (RGB) clump of He-burning stars.

However the assessment of the reality of this feature is complicated by field star contamination.

The first step of the cleaning procedure is to select probable cluster members according to the distance from the nominal cluster center. To this aim we performed a star count analysis, counting the number of stars falling in concentric area-normalized annuli 0.5 arcmin wide, centered on the clus-

ter center. The result is shown in the upper panel of the same figure. Here the dashed line is the level of the field estimated from star counts in a region 7 arcmin apart from the cluster center. Interestingly we find that the cluster is larger than previous estimates, and suggest that the radius of Trumpler 23 is about 5.0 arcmin, and it is defined as the distance from the cluster center where star counts reach the field level. The shape of the radial density profile is already an evidence of the cluster reality. The second step is to consider as probable cluster members all the stars falling inside the cluster radius (mid-left panel), and as field stars all the stars lying beyond 7 arcmin from the cluster center in a equal area field (mid-right panel). Now, we proceed to clean the CMD, by adopting the following technique. For any field star in the field CMD, we look for the closest cluster star in the cluster CMD, and remove it from the cluster CMD. This procedure in principle takes into account the different field and cluster completeness, although in this case this is not an issue, being cluster and field inside the same frame. The result is shown in the right panel of Fig. 8.

The following considerations can be made:

- The MS and the TO region in this panel are much better defined; in particular the MS is quite narrow indicating a modest field star contamination down to $V \approx 20.0$. A few stars located above the TO could be Blue Stragglers, common in open star clusters (Ahumada & Lapasset 1995), or interlopers;
- There is a nice clump of stars at $V=14.80$, $(V-I)=2.0$, similar to the clump observed in open clusters like NGC 2477 (Kassis et al. 1997) or NGC 6583 (Carraro et al. 2005a).
- The fine structure of the MS deserves further attention, since a binary stars may concur to blur this region.

Finally, the detailed shape of the TO deserves some attention. In fact the shape of the TO is that one typical of intermediate-age open clusters, with red hook (the MS termination point) clearly visible, notwithstanding some field and binary star contamination. Again, the shape of the TO and the presence of a clump indicate an age in the range 0.5-1.5 Gyr, depending on the metallicity. A preliminary estimate of the cluster age can be derived by using the Carraro & Chiosi (1994) calibration, which is based on the magnitude difference ΔV between the TO and the mean clump magnitude. In this case ΔV is about 0.8-1.0 mag., which implies an age around 1 Gyr, depending on the metallicity of Trumpler 23.

To derive the cluster fundamental parameters, we make use of the comparison between the stars distribution in the CMD and a set of theoretical isochrones from the Padova group (Girardi et al. 2000). We already have an indication of the cluster age, but we lack information about the reddening, distance and the metallicity.

The results of the fits are shown in Fig. 9. In the left panel we present Trumpler 23 clean CMD and superimpose isochrones of 0.5, 0.6 and 0.8 billion years for a solar ($Z=0.019$) metallicity. The fit is quite good both along the MS, in the TO and in the evolved stars region for the 0.6 billion years isochrone.

We achieved this results by shifting the isochrone with $E_{(V-I)} = 1.05 \pm 0.05$ ($E_{(B-V)} = 0.84$), and $(m-M)_V = 14.35 \pm 0.20$ (errors by eye).

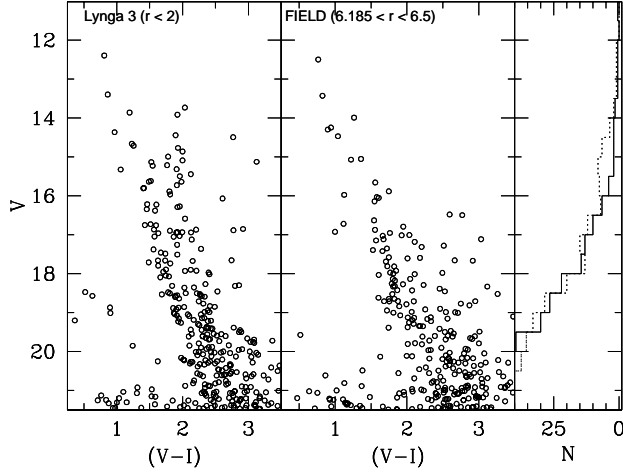


Figure 10. V vs $(V-I)$ CMDs of Lynga 3 as a function of radius from the adopted cluster center. **Left panel:** the cluster area, derive inspecting Fig. 2. **Middle panel:** the field area. **Right panel:** histograms of the cluster (dotted line) and the field (solid line)

The right panel shows our fit for $Z=0.008$, and for ages of 0.5, 0.7 and 0.8 Gyrs. The best fit is achieved with the 0.7 billion years isochrone, and implies $E_{(V-I)} = 1.15 \pm 0.05$ ($E_{(B-V)} = 0.92$), and $(m-M)_V = 14.25 \pm 0.20$. The fits in the two panels are comparably good, and therefore we conclude that the cluster age is about 0.7 ± 0.1 Gyrs, while the cluster reddening is 1.10 ± 0.10 . As for the distance modulus, we adopt 14.30 ± 0.20 .

As a consequence, Trumpler 23 turns out to be located about 2.2 kpc from the Sun, in the Fourth Galactic Quadrant. This implies a distance from the Galactic center of 6.7 kpc and a height of 16 pc below the Galactic plane.

3.2 Lynga 3

This cluster was first noted by Lynga (1964). It is identified by a concentration of a few bright stars (see Fig. 2) in the direction of the Carina spiral arm. We inspected the 2MASS catalogue to see whether in the K_s image an overdensity appears, but this does not show any cluster at the limiting magnitude of the image. The CMD of the apparent overdensity (Fig. 10, left panel) does not show any significant difference with respect to a comparison field (Fig. 10, mid panel). The putative MS has the same mean color and slope of the field apart from a vertical group of stars at $(V-I) \approx 2$ and $13.8 \leq V \leq 16.0$. This is readily visible also in the right panel of the same figure, where the dotted line is the cluster histogram, and the solid line the field histogram. The two histogram are indeed identical but for the aforementioned group of stars.

We argue that Lynga 3 is not a cluster, but an over-density of a few bright stars probably located inside the Carina arm.

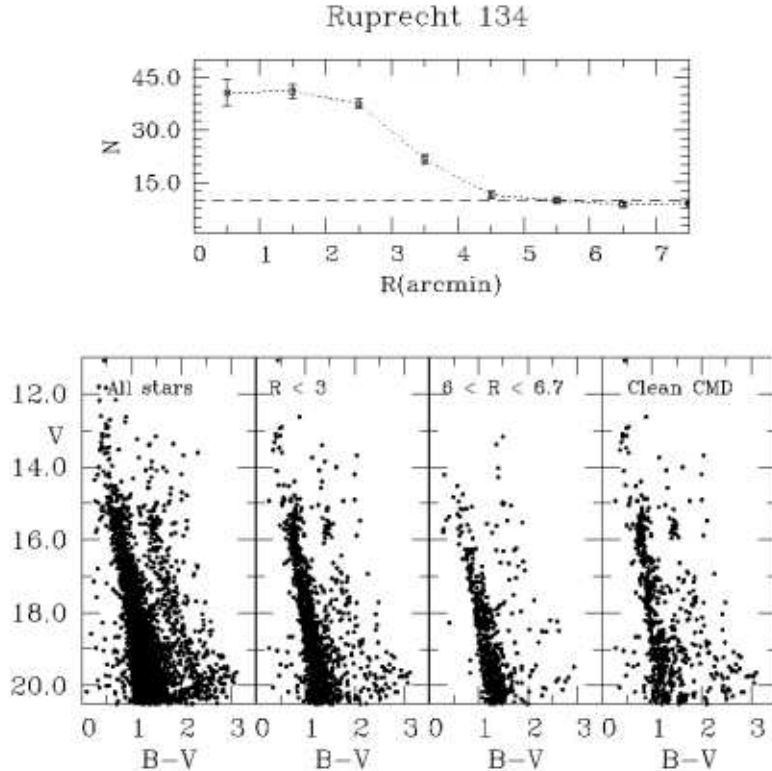


Figure 12. The open cluster Ruprecht 134. The upper panel shows the radial density profile, while the lower panels, from the left to the right show the CMD of all the observed stars, and of the cluster, field and field-decontaminated cluster, respectively. See text for more details.

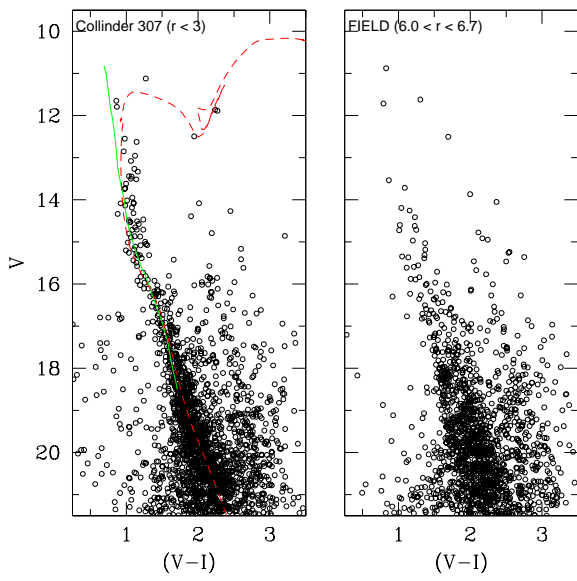


Figure 11. V vs $(V - I)$ CMDs of Collinder 307 as a function of radius from the adopted cluster center.

3.3 Collinder 307

This cluster was discovered by Collinder (1931) and then by van den Bergh & Hagen (1975), who named it BH 193,

and described it as a poorly populated cluster having a diameter of 6 arcmin, clearly visible both on red and on blue plates (see Fig. 3). Moffat & Vogt (1975) obtained UBV photometry of a few stars, which turned out to be red, and concluded that there was no evidence of a star cluster in that direction. The 2MASS K_s image we inspected shows beyond any doubt a sparse cluster at the limiting magnitude of the image. We construct the CMD as a function of the distance from the adopted cluster center, although it is clear from Fig. 3 that the cluster occupies all the region we observed, and for this reason we are not going to provide a radial density profile. Left panel of Fig. 11 shows the cluster area, namely all the stars lying within 3 arcmin from the cluster center, whereas the right panel shows a blank field extracted from the outskirts of the CCD image. The cluster clearly exists, with a distinct MS extending from $V = 13$ down to $V = 20$. The slope of the MS demonstrates that the cluster is relatively young. We superposed an empirical Schmidt-Kaler(1982) ZAMS (solid line) which fits the bulk of the stars adopting $E(V-I) = 1.05$ ($E(B-V) = 0.84$) and $(m - M)_V = 13.4$. This implies that the cluster lies at 1.3 kpc from the Sun, and 60 pc below the Galactic plane, well inside the Carina-Sagittarius spiral arm. A solar metallicity isochrone shifted by the same reddening and distance modulus (dashed lines) yields a nice fit for an age of 250 Myr.

3.4 Ruprecht 134

This clustering is reported by Ruprecht (1966) who assigns to it Trumpler (1929) type *III 1 p*, say a poorly populated sparse open cluster (see Fig. 4). In this figure the cluster appears as a clump of bright stars. The northern part of the field is dominated by a conspicuous dust lane. We inspected also for this cluster a 2MASS K_s image, and actually we can see a sparse distribution of a few bright stars, which indicates a possible star cluster.

To assess the cluster reality we employ the same technique we used for Trumpler 23, and the results are presented in Fig. 12.

The left panel presents the CMD of all the stars in the covered field. We built up the cluster CMD considering the stars located within 3 arcmin from the cluster nominal center (Table 1) and estimating the field star contamination in a equal area ring located in the outskirts of the surveyed field. This choice was driven by the appearance of the cluster radial density profile (see the upper panel of Fig. 12): it is readily seen that the cluster reaches the level of the field at a distance of about 4.0-4.5 arcmin.

The two CMDs are shown in the middle-left and middle-right panels of Fig. 12. The CMD of the field decontaminated cluster is shown in the right panel of the same figure. This panel shows a tight MS and a clump of stars at $V = 15.5$, $(B-V) = 1.5$. This clump in the middle-right panel is not as visible as the cluster clump, and the MS is more scattered and terminates 1.5 mag. fainter than in the cluster. We interpret these facts as signatures of the existence of a intermediate age star cluster, very similar to Trumpler 23 (see Fig. 8).

To derive the cluster fundamental parameters we super-pose a solar metallicity isochrone, shifted by $E(B-V) = 0.5$ and $(m - M)_V = 14.2$, which provides a reasonable fit of the TO and clump region for an age of 1.0 Gyr (see Fig. 13). We tried younger ages to better match the clump position. However by decreasing the age only by a few million years the theoretical clump gets too red compared with the observed one, and for this reason we exclude ages significantly younger than 1.0 Gyr. In turn, this yields a distance of 3.4 kpc from the Sun exactly toward the Galactic Center, and a Galactocentric distance of 5.2 kpc. As for Trumpler 23, we are facing here a really interesting object, which deserves further attention due to its unusual combination of age and position in the Galaxy.

3.5 ESO552SC16

This asterism is included in the ESO/Uppsala catalogue (Lauberts 1982) and is a very compact clustering embedded in a rich stellar field (see Fig. 5). The 2MASS K_s image which we inspected does not show any cluster at the limiting magnitude of the image. The CMD of the apparent over-density (Fig. 14, left panel) does not show any significant difference when selecting different areas of the CCD frame. We conclude that ESO552SC16 is not a physical cluster. Interestingly, we detect an almost vertical sequence at $(V-I) \approx 2.0$, $19 \leq V \leq 15$. This is clearly a sequence of young stars evenly distributed across the covered field. A fit with the empirical Schmidt-Kaler ZAMS yields a heliocentric dis-

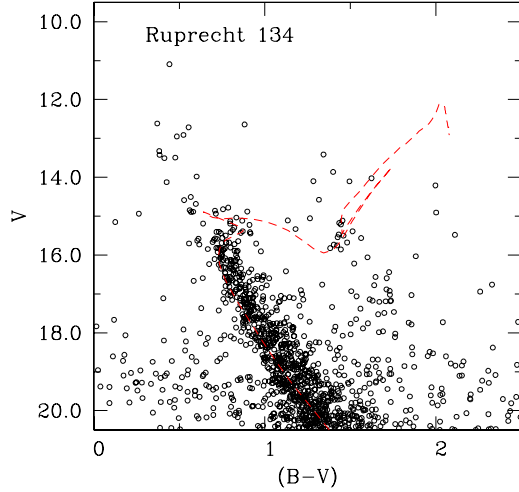


Figure 13. Isochrone solution for the cluster Ruprecht 134. The 1 Gyr solar metallicity isochrone has been shifted by $E(B-V)=0.5$ and $(m - M)_V=14.2$

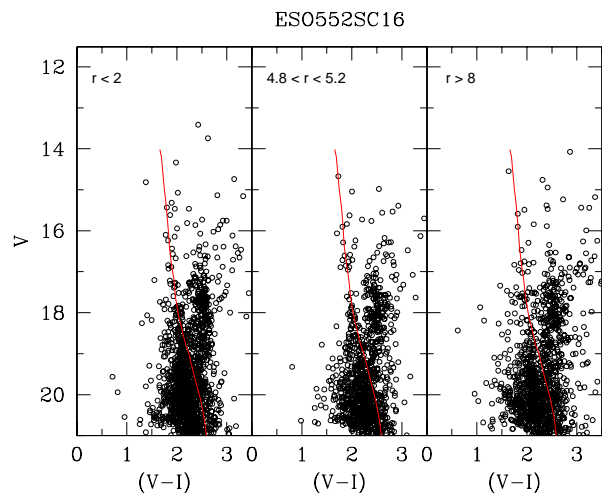


Figure 14. V vs $(V-I)$ CMDs of ESO552SC16 as a function of radius from the adopted cluster center. The superposed ZAMS has been shifted by $(m - M)_V = 16.6$ and $E(V-I) = 1.90$

tance of 2.2 kpc ($E(V-I) = 1.9$ and $(m - M)_V = 16.6$) and a height below the plane of about 200 pc. The Galactic position of this young population is compatible with the pattern of the Carina-Sagittarius spiral arm. The apparent over-density in the direction of ESO552SC16 which looks like a compact cluster is probably an extinction effect.

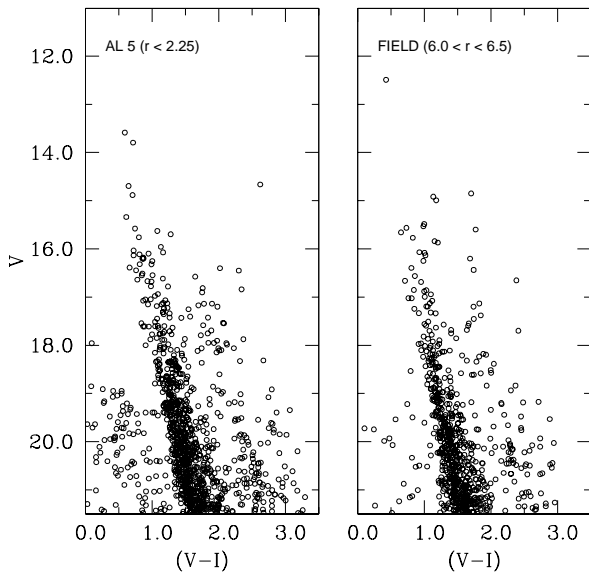


Figure 15. V vs $(V - I)$ CMDs of AL 5 as a function of radius from the adopted cluster center. The CMDs refer to two equal area fields.

3.6 AL 5

This cluster was discovered by Andrews & Lindsay (1967) who describe it as a circular ensemble of faint stars with a diameter of 2.25 arcmin (see Fig. 6). The 2MASS K_s image does not show a cluster at the limiting magnitude, and the DSS B image neither. The impression of a cluster is the results of the patchy extinction pattern in the region. We then build up CMDs as a function of stars' distance from the nominal cluster center. The CMD (see Fig. 15) of the apparent over-density (left panel) does not show any significant difference with respect to a comparison field (right panel). The putative Main Sequence has the same mean color and slope of the field. We believe that the small difference in the number of stars is simply an absorption effect. We conclude that there is no cluster in the direction of AL 5.

3.7 Kronberger 3

This small clustering (see Fig. 7) has been identified by Matthias Kronberger, who already suggested to be an asterism, and not a real cluster (private communication to Wilton Dias, ¶). Both the inspection of the 2MASS image and the global appearance of the CMD (see Fig. 16) strengthen the impression that Kronberger 3 is just a random group of stars. In fact the CMD of the putative cluster does not differ from the that of surrounding field. We therefore conclude that Kronberger 3 is not an open cluster.

¶ <http://www.astro.iag.usb.br/~wilton/removed.txt>

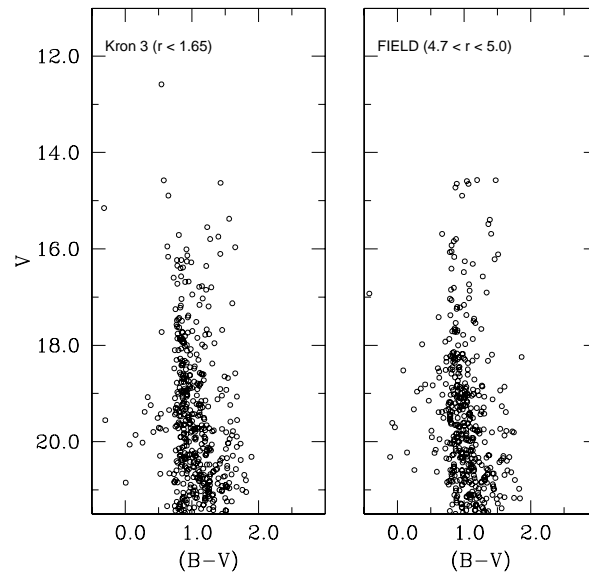


Figure 16. V vs $(V - I)$ CMDs of Kronberger 3 as a function of radius from the adopted cluster center. The CMDs refer to two equal area fields.

4 DISCUSSION AND CONCLUSIONS

The derived parameters of the program clusters are listed in Table 2. Together with reddening, distance, age and the corresponding uncertainties, we list the Galactocentric distance, derived by assuming $R_\odot = 8.5\text{kpc}$ and the Galactocentric rectangular coordinates X_\odot , Y_\odot and Z_\odot . The adopted reference system is centered on the Sun, with the X and Y axes lying on the Galactic plane and Z perpendicular to the plane. X points in the direction of the Galactic rotation, being positive in the first and second Galactic quadrants; Y points toward the Galactic anti-center, being positive in the second and third quadrant; finally, Z is positive toward the north Galactic pole (Lynga 1982).

Trumpler 23 and Ruprecht 134 are two very interesting clusters of intermediate age located inside the solar ring which, together with NGC 6404 and NGC 6583 (Carraro et al 2005a) and AL 1 (Carraro et al. 2005b), significantly increase the number of open clusters of that age known to lie so close to the Galactic center. Future spectroscopic programs should consider these clusters since they would allow to enlarge the baseline of the Galactic disk radial abundance gradient by more than 2 kpc. Furthermore, Trumpler 23 (see Fig 1) has an elongated shape which might indicate that it is undergoing strong tidal interaction with Milky Way.

Collinder 307 results to be a 250 Myr old cluster located 100 pc below the Galactic plane, in the Carina-Sagittarius spiral arm.

All the other clusters are just visual effects, accumulations of stars produced by the patchy nature of the interstellar absorption toward the Galactic bulge.

This work highlights the difficulties of working with

Table 2. Parameters of the studied clusters. The coordinate system is such that the Y axis connects the Sun to the Galactic Center, while the X axis is positive in the direction of galactic rotation. Y is positive toward the Galactic anti-center, and X is positive in the first and second Galactic quadrants (Lynga 1982).

Name	$E(B - V)$	$(m - M)_V$	d_\odot	X_\odot	Y_\odot	Z_\odot	R_{GC}	Age
	mag	mag	kpc	kpc	kpc	pc	kpc	Myr
Trumpler 23	0.85±0.05	14.3±0.2	2.2	-1.1	-1.9	-16	6.7	1000±200
Lynga 3	Spiral arm							
Collinder 307	0.84±0.10	13.4±0.2	1.3	-1.6	-0.8	-60	6.9	250±50
Ruprecht 134	0.50±0.05	14.2±0.2	3.4	0.0	-3.4	-100	5.2	1000±200
ESO552SC16	spiral arm							
AL 5	No cluster							
Kronberger 3	No cluster							

open clusters toward the inner regions of the galaxy. The star densities are large, and increase rapidly with distance. That causes the appearance of a main sequence on all of the CMDs in this paper, resulting simply from the geometry of the situation. Furthermore, patchy obscuration is likely to play a role in creating apparent “clusters” that are not physical associated groups of stars.

Nevertheless, in recent works (Carraro et al 2005a,e) we have discovered a considerable number of neglected intermediate-age open clusters, which are going to significantly modify the open cluster age distribution and probably the typical open cluster lifetime as presently known.

ACKNOWLEDGEMENTS

The observations presented in this paper have been carried out at LCO, CTIO and LSO, Chile. CTIO is operated by the Association of Universities for Research in Astronomy, Inc. (AURA), under a cooperative agreement with the National Science Foundation as part of the National Optical Astronomy Observatory (NOAO). The work of G. Carraro is supported by *Fundación Andes*. R. A. Méndez and E. Costa acknowledge support from the Chilean *Centro de Astrofísica* FONDAP No. 15010003. G. Carraro thanks Ricardo Salinas and Marcio Catelan for securing part of the observations described in this paper. This study made use of Simbad and WEBDA databases.

REFERENCES

- Ahumada J., Lapasset E., 1995, A&AS 109, 375
 Andrews A.D., Lindsay E.M. 1967, Irish Astron. Journal 8, 126
 van den Bergh S., Hagen G.L. 1975, AJ 80, 11
 Bertelli G., Nasi E., Girardi L., Chiosi C., Zoccali M., Gallart C., 2003, AJ 125, 770
 Carraro G., Chiosi C., 1994, A&A 287, 761
 Carraro G., Mendez R.A., Costa E., 2005a, MNRAS 356, 647
 Carraro G., Janes K.A., Eastman J.D., 2005b, MNRAS, 364, 179
 Carraro G., Geisler D., Moitinho A., Baume G., Vázquez R.A., 2005c, A&A 442, 917
 Carraro G., Baume G., Piotto G., Mendez R.A., Schmidtbreick L., 2005d, A&A 436, 527
 Carraro G., Baume G., Vázquez R.A., Moitinho A., Geisler D., 2005e, MNRAS 362, 649
 Collinder P., 1931, Ld. An., 2
 Friel E.D., Janes K.A., Tavarez M., et al., 2002, AJ 124, 2693

- Girardi L., Bressan A., Bertelli G., Chiosi C., 2000, A&AS 141, 371
 Janes K.A., Phelps R.L., 1994, AJ 108, 1773
 Kassis M., Janes K.A., Friel E.D., Phelps R.L., 1997, AJ 113, 1723
 Landolt A.U., 1992, AJ 104, 340
 Lauberts A., 1982, the ESO/Uppsala Survey of the ESO(B) Atlas
 Lynga G., 1964, Lund Medd. Astron. Obs. Ser. II, 140, 1
 Lynga G., 1982, A&A 109, 213
 Moffat A.F.J., Vogt N., 1975, A&AS 20, 155
 Patat F., Carraro G., 2001, MNRAS 325, 1591
 Ruprecht J. 1966, BAICz 17, 33
 Schmidt-Kaler, Th. 1982, Landolt-Börnstein, Numerical data and Functional Relationships in Science and Technology, New Series, Group VI, Vol. 2(b), K. Schaifers and H.H. Voigt Eds., Springer Verlag, Berlin, p.14
 Stetson P.B. 1987, PASP 99, 191
 Trumpler R.J. 1929, PASPL 1, 89